Recognition of Anionic Porphyrins by DNA Aptamers†

Yingfu Li, C. Ronald Geyer, and Dipankar Sen*

Institute of Molecular Biology and Biochemistry, Simon Fraser University, Burnaby, British Columbia V5A 1S6, Canada

Received January 4, 1996; Revised Manuscript Received March 5, 1996⊗

ABSTRACT: DNA sequences were isolated by *in vitro* selection for binding to *N*-methylmesoporphyrin IX (NMM), a molecule that behaves as a stable transition-state analogue for porphyrin chelatases. Clones ∼280 and ∼120 nucleotides long were obtained, which bound to NMM with sub-micromolar affinity but bound mesoporphyrin IX (MPIX), as well as various metalloderivatives of MPIX, with lower affinity. Footprinting experiments with dimethyl sulfate, DNase I, and bound hemin molecules activated by superoxide identified a series of short guanine-rich motifs to be the binding sites for the various porphyrins. One clone, **PS2**, examined in depth, gave a methylation footprint with bound NMM but not with bound MPIX nor with a number of metalloporphyrins. The binding domain of **PS2**, synthesized as a short oligonucleotide, itself showed high-affinity binding to NMM. The binding sequences from different clones were loosely homologous, and the footprinting data were consistent with their folding to form one or more guanine quartets in the presence of NMM. Ultraviolet−visible absorption and circular dichroism spectroscopy of the DNA−NMM complexes indicates, however, that the interaction is not primarily intercalative in nature. The preferential binding of NMM by these aptamers raises the possibility of their being able to catalyze the chelation of metal ions by the porphyrin MPIX.

Porphyrins and metalloporphyrins are found widely in nature and are used by organisms as cofactors for a variety of enzymes and other specialized proteins. Metalloporphyrins are extraordinarily versatile and participate in oxygen transport, electron transfer, and a variety of redox chemistries, such as those associated with catalases, peroxidases, and monooxygenases. Although a variety of protein−porphyrin complexes and conjugates exist in nature, no functional role *in vivo* has yet been attributed to porphyrin−nucleic acid complexes; indeed, naturally occurring anionic porphyrins have not been found to associate with double-helical RNA or DNA, either *in vivo* or under experimental conditions *in vitro*. Recently, however, a class of synthetic cationic porphyrins, including mesotetra(4-*N*-methylpyridyl)porphine (T4MPyP), containing two or more positive charges, has been found to bind double-helical DNA [reviewed by Fiel (1989), Gibbs et al. (1988), and Marzilli (1990)].

The interaction of such cationic porphyrins with DNA appears to follow, under different conditions, one of three modes: intercalation between the DNA base pairs, outside binding, and outside binding reinforced by self-stacking interactions between the porphyrins. The cationic porphyrin−DNA interactions have been studied extensively, using a wide variety of spectroscopic and footprinting techniques, and have been subjected to kinetic and thermodynamic analyses [reviewed by Fiel (1989)]. The utility of these interactions has been seen in terms of their potential for (a) *in vivo* photodynamic therapy [a variety of porphyrins have been found to photosensitize DNA strand cleavage, and this property has been used and is currently being developed for the treatment of certain cancers [reviewed by Marzilli (1990)]] and (b) use as analytical probes for investigating higher-order structures formed by nucleic acids, particularly branched DNA and RNA structures (Lu et al., 1990; Nussbaum et al., 1994).

A quite distinct rationale for studying porphyrin−DNA (or −RNA) interactions is to test whether it is possible for single-stranded RNAs or DNAs to fold to create specific binding pockets for different porphyrins, including those, such as anionic porphyrins, which do not naturally bind to nucleic acids. Recently, *in vitro* selection techniques have been used to isolate from large (10^{14}−10^{15}) pools of single-stranded and random RNA and DNA sequences molecules that bind a variety of target molecules [reviewed recently by Szostak (1993), Joyce (1994), and Hirao and Ellington (1995)]. The targets include small molecules, such as dyes (Ellington & Szostak, 1990, 1992); amino acids (Famulok & Szostak, 1992; Connell et al., 1993); cofactors such as cyanocobalamin (Lorsch & Szostak, 1994), flavin, and nicotinamide (Lauhon & Szostak, 1995); bases and nucleotides (Sassanfar & Szostak, 1993; Jenison et al., 1994; Huizenga & Szostak, 1995); as well as proteins (Tuerk & Gold, 1990; Tuerk et al., 1990, 1992; Bock et al., 1992; Jellinek et al., 1993, 1994). The specifically binding nucleic acids, or "aptamers" (Ellington & Szostak, 1990), have been found in a number of instances to bind their targets with sub-micromolar affinity.

We tested first whether it was possible to isolate DNA aptamers for anionic porphyrins. The large, aromatic ring structures of porphyrins should make them attractive targets for binding by specific DNA secondary/tertiary structures. The first published reports on DNA and RNA aptamers had, in fact, described the isolation of molecules that bound polycyclic dyes (Ellington & Szostak, 1990, 1992).

A second question was that, if indeed anionic porphyrin-binding DNA aptamers could be isolated, would these aptamers be able to distinguish between homologous porphyrins with subtle structural differences? This question relates to naturally occurring ferrochelatase enzymes, which catalyze the insertion of Fe^{2+} ions into protoporphyrin as a

† This work was supported in part by the National Science and Engineering Research Council of Canada (NSERC). D.S. is a Research Scholar of the British Columbia Health Research Foundation (BCHRF).

⊗ Abstract published in *Advance ACS Abstracts,* May 1, 1996.

S0006-2960(96)00038-4 CCC: $12.00

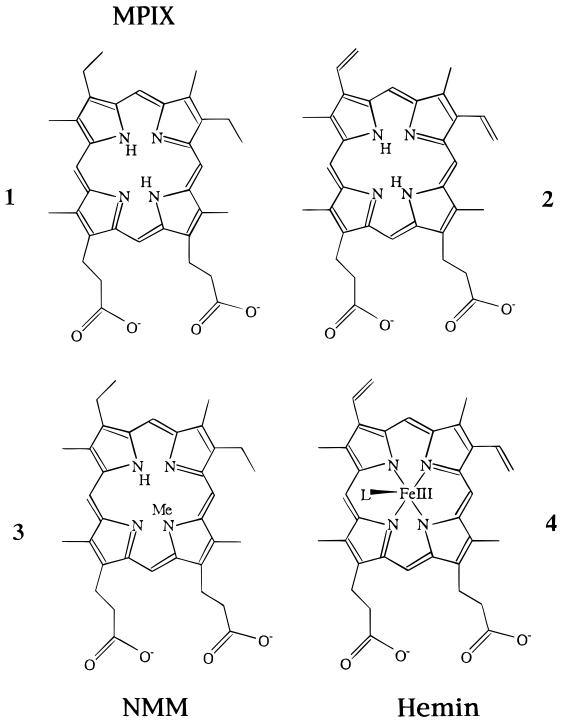

FIGURE 1: Porphyrins used in this study: **1**, mesoporphyrin IX (MPIX); **2**, protoporphyrin IX; **3**, *N*-methylmesoporphyrin IX (NMM); and **4**, hemin [iron(III) protoporphyrin IX]. L refers to an axial ligand, which is Cl or OH (possibly the latter under our experimental conditions).

key step in the biosynthetic pathway to heme (Lavallee, 1988). The bent porphyrin *N*-methylprotoporphyrin IX has been found to be a potent inhibitor of this enzyme, possibly because it resembles the transition state for the insertion of metal ions into its natural substrate, protoporphyrin IX (Dailey & Fleming, 1983). This property was taken advantage of by Cochran and Schultz (1990a) to generate catalytic antibodies [reviewed by Schultz and Lerner (1995)] that mimicked ferrochelatase. Cochran and Schultz obtained monoclonal antibodies by immunizing mice with the bent *N*-methylmesoporphyrin (NMM); two of these antibodies were then found to catalyze the insertion of Zn^{2+}, Co^{2+}, Mn^{2+}, and Cu^{2+} into the planar mesoporphyrin IX (MPIX). Figure 1 illustrates the structures of protoporphyrin IX, mesoporphyrin IX (MPIX), *N*-methylmesoporphyrin (NMM), and hemin [iron(III) protoporphyrin IX].

Given this, it is possible to pose the question that if discriminating aptamers could be isolated, which bound with higher affinity to NMM than to MPIX, whether such aptamers would then show chelatase-like activity.

The *in vitro* selection technologies used to obtain nucleic acid aptamers are unique in the sense that DNA or RNA molecules can be selected in a positive sense for binding to a given target, A, and then subjected to negative selections for binding to closely related molecules, B−D. That aptamers can be highly discriminating for recognition and binding of closely related structures was notably demonstrated with RNA molecules that discriminated between caffeine and theophylline (Jenison et al., 1994). Since then, other examples have been reported.

A third point of potential interest relates to the general and broad importance of porphyrins as cofactors for proteins found in modern organisms. It may be reasonable to assume that in the evolution of life on earth there was an "RNA world" (White, 1976; Gilbert, 1986; Benner et al., 1989). It is conceivable that, in such an RNA world, RNAs catalyzing metabolically important redox reactions might have recruited porphyrins or porphyrin-like molecules as cofactors.

MATERIALS AND METHODS

Materials. Porphyrins were purchased from Porphyrin Products (Logan, UT) and were used without further purification. Avidin-conjugated agarose beads and oxirane−acrylic beads were from Sigma. Deoxynucleotide triphosphates (dNTPs) and the T7 Sequencing Kit were from Pharmacia. [γ-^{32}P]ATP (3000 Ci/mol) was from Amersham. T4 polynucleotide kinase, T4 DNA ligase, *Bam*HI, *Hin*dIII, *Pvu*II, and DNase I were from BRL. *Ban*I and *Sty*I were from New England Biolabs. *Taq* DNA polymerase was from Perkin-Elmer. Bluescript M13$^+$ plasmid and MC1061 competent *Escherichia coli* were gifts of Dr. C. Boone at Simon Fraser University; the "random" DNA oligomers (R1 and R2) and biotinylated oligonucleotide primers were synthesized at the University Core DNA Services at the University of Calgary.

DNA Library. The random-sequence DNA library used in this work was constructed according to the method of Bartel and Szostak (1993), with minor modifications. Two synthetic polynucleotides, R1 (5′-TTGATCCGGTC*GGCACC*-N_{76}- CCTTGGGTCATTAGGCGA) and, R2 (5′-CGG-GACTCTGACCTTGG-N_{76}- *GGCACC*TGTCCACGCTC), were each rendered double-stranded by PCR. R1 was divided into two pools and restriction-digested, one pool with *Ban*I (cutting at *GGCACC*) and the other with *Sty*I (cutting at CCTTGG); R2 was digested with both enzymes. A 2-fold ligation was then carried out with T4 DNA ligase, to give duplexes of the form R1−R2−R1, containing a total of 228 random base pairs (bp). Ligated product (540 μg) was obtained, corresponding to 1.8×10^{15} different molecules. This library was then amplified with a large-scale (500 mL) PCR, using the primers R1P1−biotin (5′-biotin-TCGC-CTAATGACCCAAGG) and RLS (5′-GGATCTTTTTGATC-CGGTCGGCACC).

Single-stranded DNA was purified from these amplified sequences by allowing the biotinylated duplexes to bind to avidin−agarose beads (avidin:biotin = 10:1). After being washed with 15 volumes of avidin column buffer [50 mM Tris (pH 7.4), 200 mM NaCl, and 0.1 mM EDTA] to remove nonbiotinylated duplexes, the unbiotinlyated strand of bound duplexes was recovered with 3 column volumes of 0.2 M NaOH. The eluant was neutralized immediately with 0.2 M HCl + 0.5 M Tris and the DNA recovered by ethanol precipitation. A total of 7.14 mg of ssDNA was obtained, corresponding to ~26 library equivalents.

The final, 283-nucleotide, single-stranded DNA had the sequence 5′-GGATCTTTTTGATCCGGTCGGCACC-N_{76}-CCTTGG-N_{76}-GGCACC-N_{76}-CCTTGGGTCATTAG-GCGA.

Selection Columns. NMM selection columns were prepared by the derivatization of oxirane−acrylic beads with *N*-methylmesoporphyrin IX (NMM). The beads were allowed to react with NMM in 0.1 M phosphate buffer (pH 4.0) for 48 h in the dark at room temperature. The disappearance of NMM with time was monitored by HPLC. After 48 h, the NMM was attached quantitatively to the beads (10 column volume washes with 0.2 M NaOH washed off

less than 2% of the NMM from the column). After the completion of the attachment reaction, the column was washed with 1 M Tris (pH 8.0) and incubated for a further 48 h with 4% mercaptoethanol to inactivate unreacted epoxy groups. Finally, the column was equilibrated with SB buffer [100 mM Tris-acetate (pH 7.4), 200 mM sodium acetate, 25 mM potassium acetate, 10 mM magnesium acetate, 0.5% Triton X-100, and 5% dimethyl sulfoxide]. Columns treated in this way were found to have very low nonspecific binding of single-stranded DNA (<1%).

To obtain blocked column material for negative selections, the oxirane beads were allowed to react with excess mercaptoethanol at pH 8.0 for 48 h and then assayed for their level of nonspecific ssDNA binding. This was also found to be low (<1%).

Selection Protocols. The NMM columns were washed and preequilibrated in SB buffer. To further reduce the nonspecific binding of single-stranded DNA molecules to these columns, an initial negative selection was carried out on a "negative column", which contained oxirane−acrylic beads inactivated with mercaptoethanol (as above). For a given round of selection, 5′-end-labeled ssDNA was denatured in TE buffer at 90 °C for 5 min and then allowed to cool slowly (over 1 h) to room temperature. The solution was subsequently made up to SB buffer.

The folded DNA samples in SB were treated to a 100 μL negative column (containing no attached NMM); the DNA was allowed to equilibrate with the column for 30 min, after which the unbound DNA was washed directly onto a 400 μL NMM column with 3 volumes of SB buffer, in which it was incubated with the NMM column for 2−3 h at room temperature. Unbound DNA was washed away with SB buffer until no more radioactivity could be detected in the washes.

In round 1, a total of 3.0 mg of DNA was applied to a 4 mL NMM column. In rounds 2 and 3, ∼100 μg of DNA was used; from the 4th to the 12th rounds, 20−50 μg of DNA was applied. While in the first three rounds TE′ buffer [10 mM Tris (pH 7.4) and 10 mM EDTA] had been used to elute the specifically bound DNA molecules from the NMM column, in rounds 4−6, high concentrations of free NMM (2.1 mM) were used to compete the DNA away from column-bound NMM (column NMM concentration = 0.5 mM). In round 6, the DNA was applied to NMM columns twice in succession; in rounds 7−12, a "negative" elution with free MPIX (0.1 mM) was used on the bound DNA prior to "positive" elution with free NMM, as above. This was done to eliminate those NMM-binding DNA molecules that also bound with high affinity to MPIX.

PCR. PCR was carried out in the following buffer: 10 mM Tris (pH 8.3−9.3), 50 mM KCl, 2.5−10 mM $MgCl_2$, 0−5% glycerol, 0.2 mM of each dNTP, 1 unit of *Taq* polymerase, 1 μM of each primer (RLS and R1P1−biotin), and 0.01−0.05 μM 5′-^{32}P-labeled RLS, for each 100 μL of the PCR solution. Reactions were usually carried out in 100−300 μL volumes. In the later rounds of selection, PCR yields were consistently low, owing presumably to the formation of strong secondary structures in the DNA molecules being enriched; therefore, the PCR conditions were reoptimized before each new round, generally by changing one of three parameters: buffer pH, $MgCl_2$ concentration, and glycerol concentration. The amplified DNA was phenol/chloroform extracted, ethanol precipitated, and bound to avidin columns for the generation of single strands (see above). In most rounds, the single-stranded DNA obtained was further purified by preparative gel electrophoresis before being subjected to a new round of selection.

Cloning and Sequencing. Following the completion of 12 rounds of selection on NMM columns, the DNA pool was amplified for cloning by PCR amplification with the following two "cloning" primers: RLC (5′-CTTGTCTG-CAG**GGATCC**TTTTGATCCGGTCGGC) and R1P1C (5′-G A T A T C **A A G C T T** C T C G A G T C G C C T A A T-GACCAAGG). The bold sequences show *Bam*HI and *Hin*dIII sites, respectively. The PCR products were gel-purified, digested with the above enzymes, and gel-purified again prior to ligation to the *Bam*HI- and *Hin*dIII-digested and gel-purified large piece of the Bluescript $M13^+$ plasmid. MC1061 competent cells were transformed with the ligation mixtures. Sixty recombinant clones were picked for the long sequences (**P** series) and fifty that contained the shorter sequences (**PS** series; see Results). Twenty-four clones of the **P** series and 24 of the **PS** series were sequenced (the **P** clones in both directions) by the dideoxy method, using a T7 Sequencing Kit (Pharmacia).

Dissociation Constant Determinations. The binding affinities of different aptamers to NMM and, indirectly, to other porphyrins, were measured using the methodology of Connell et al. (1993). ^{32}P-labeled DNA was applied in SB buffer to a 0.1 mL NMM column, allowed to equilibrate for 30 min, and then quickly washed with a few column volumes of SB buffer until the unbound DNA had been washed away. Specific elutions were then carried out with solutions of 100 μM NMM as well as with solutions of other porphyrins, in SB. K_d was calculated according to the formalism $K_d = L[(V_{eL} - V_n)/(V_e - V_{eL})]$ (Connell et al., 1993), where L was the concentration of the free ligand in solution, V_{eL} the elution volume in the presence of free ligand in solution, V_e the buffer elution volume in the absence of free ligand, and V_n the void volume of the column (taken to be 70% of the volume of the packed column).

Footprinting. Final DNA concentrations used in all footprinting experiments were between 1 and 3 ng/μL. Reactions were carried out in SB buffer at room temperature, unless otherwise specified. Single-stranded aptamer DNAs were 5′-end-labeled with polynucleotide kinase and [γ-^{32}P]-ATP and gel-purified. The DNA was denatured and then allowed to fold in SB buffer, as above. Porphyrins were prepared as stock solutions in SB buffer. Final DNA−porphyrin complexes were made up by combining appropriate aliquots of the DNA and porphyrin stocks, which were then made up with SB buffer to final volumes of 15 μL (for DMS methylation) and 10 μL (for hemin/KO_2 and DNase I cleavages).

Methylation Protection. Aliquots (0.8 μL) of freshly made 2% dimethyl sulfate (DMS) in double-distilled water were added to the 15 μL DNA−porphyrin solutions. Samples were incubated at room temperature for 30 min and then ethanol precipitated. The pellets were washed and treated with piperidine using standard Maxam−Gilbert protocols, and the cleaved DNA was analyzed in 10−20% denaturing polyacrylamide gels.

Hemin/KO_2 Footprinting. Aliquots (2.5 μL) of a freshly made solution of 150 mM KO_2 in SB were added to 10 μL DNA−porphyrin samples. These were incubated at 37 °C for 30 min, and the reaction was quenched by adding 6 μL

of formamide gel-loading buffer and heating at 85 °C for 3 min (Ward et al., 1986). One-fifth portions of the samples were analyzed in 10−15% denaturing polyacrylamide gels.

DNase I Footprinting. These experiments were carried out under conditions similar to those of the hemin/KO_2 experiments, except that 1 μL of DNase I (from a 0.02 unit/μL stock) was added to each 10 μL DNA/NMM solution in SB buffer.

For the aptamer **PS5**, the hemin/KO_2 footprinting was carried out within gel fragments containing the aptamer. Separate samples of end-labeled **PS5**, with added hemin (0.5 mM) and without, were run in a nondenaturing gel. The gel bands containing the aptamer were cut out, crushed, and preincubated with 50 μL of 1 mM hemin in SB for 30 min at room temperature. Fifty microliters of 30 mM KO_2 in SB was then added and the mixture incubated for 30 min at 37 °C. Finally, the DNA was eluted from the gel slices and ethanol precipitated prior to running in a 15% denaturing gel.

Gel Mobility Shift Studies. Single-stranded aptamers were denatured and refolded as above and then either incubated or not incubated with 100 μM NMM for 30 min before loading in a nondenaturing polyacrylamide gel run at 4 °C in 50 mM Tris-borate + 10 mM KCl + 5 mM $MgCl_2$ buffer.

Spectroscopic Studies. The concentration of DNA used for ultraviolet−visible spectrometry was 5 μM; measurements were carried out in a dual-beam Cary 3E UV−Visible Spectrophotometer. **PS2** DNA was allowed to fold in SB buffer in the sample cuvette. This DNA solution (as well as DNA-free SB buffer in a separate cuvette) was then made progressively to 0, 1, 3, 5, 10, 15, 20, and 30 μM NMM and scanned from 300 to 700 nm (spanning the Soret and visible absorption regions of the porphyrin) in comparison with a cuvette containing only buffer, following each addition.

Circular dichroism measurements were carried out in a J-700 CD spectrometer. Folded (3 μM) aptamer (**PS2**, **ST1**) in SB buffer was first scanned in the absence of added NMM. Then, 1, 3, 5, 10, 15, 20, and 30 μM NMM were introduced, and CD spectra taken for both the DNA absorption regions (200−300 nm) and the Soret and visible absorption regions of the NMM (300−550 nm).

RESULTS

Appearance of a "Small" Porphyrin-Binding DNA Library

During the selection procedure on the 283-nucleotide DNA library, particularly in the later rounds of selection, a significantly smaller-sized DNA began to appear in large amounts following PCR amplifications of recovered DNA. In general, two sizes of DNA PCR products were always to be seen with this particular random-sequence library: one the normal-sized 283 nucleotides and the other approximately 120 nucleotides long. By the third selection, the small-sized DNA was the dominant product after 20 rounds of PCR amplification, arising, presumably, from mispriming by the primers RLS and R1P1−biotin off the two six-nucleotide constant regions (CCTTGG and GGTGCC) separating the three random regions. To correct for this situation, a separate primer, RLT, was synthesized to replace RLS (RLT lacked the last five nucleotides of RLS at the 3′-end). This improved the yield of the full-sized 283 nucleotides somewhat. However, in the later rounds of selection, it became increasingly difficult to amplify the 283-nucleotide product, even when gel purification was used to eliminate the smaller product prior to each new selection. Beyond round 10, the "small" and "large" aptamers were subjected to separate selection and PCR cycles and were cloned as distinct populations of aptamers. The "**PS**" family of clones described in this paper refers to the small aptamers and the "**P**" family to the full-sized ones.

Comparison of Aptamer Sequences

Twenty-four clones were sequenced from each size class of aptamer, to determine whether a common-sequence (and therefore folded structure) motif was responsible for the binding of NMM. Figure 2 shows the random sequences from 24 of the smaller (**PS** class) of aptamers, all of which contain the 5′-most of the three random regions present in the original 283-nucleotide library. The most notable feature of these sequences is the presence in each of a highly guanine-rich motif (bold and italicized). The pool of the larger class of aptamers (the **P** class) had similar motifs, and in some cases (such as in **P3**, described later) more than one of these motifs in a given aptamer. A rigorous comparison of the sequences using the FASTA program revealed the highest degree of homology to be present, in fact, in the guanine-rich regions, which were typically 15−30 nucleotides long. From this collection of clones, two small aptamers, **PS2** and **PS5**, and three large aptamers, **P3**, **P7**, and **P9**, were randomly selected for a more in-depth study of their properties. Most of our studies focused on **PS2**, which gave the most defined footprints. At a later stage (described below), a short oligomer, **ST1**, corresponding to the guanine-rich region of **PS2**, was also synthesized for study.

Binding Affinities

In order to determine whether the selection scheme had succeeded in enriching for DNA aptamers that preferentially bound to NMM, the binding affinities of the different DNA clones for NMM and, indirectly, for other porphyrins were measured, using the methodology of Connell et al. (1993). The equilibrium distribution of aptamer molecules between column-bound ligand and free ligand in solution was used to compute dissociation constants. Table 1 shows the dissociation constants measured for clones **PS2** and **P7**, and the oligomer **ST1**, for binding to different porphyrins. Separate measurements were taken in a number of instances, to gauge the accuracy of the K_d measurements (found to be within 80−100% accuracy). All three aptamers bound to NMM with sub-micromolar affinity, whereas their binding affinities to MPIX were reproducibly lower (by 3−8-fold), as were their affinities for a number of metalloporphyrins derived from MPIX (as well as hemin). These data indicate that the selection strategy used to enrich for these aptamers (with negative selection against MPIX followed by positive selection against NMM) was successful, to a point, in enriching for aptamers with differences in affinity for the two porphyrins. However, the discrimination between MPIX and NMM is not very large. Up to what upper limit these differences in affinity can be enhanced will be the subject of future investigations.

PS Series Sequences

ps2 TTGCC TAACC GTGAA GGTAA AACGA TTTAG TCAAA C*GTGG GAGGG CGGTG GTGTT G*ACTG ATCGA TTTTA TTCCA
ps3 AGGGT TGATC AACTA *G GGTA GTCGG GAGGT GGTGG GG*CTT GTTTG TGTCA GCCTG CAGTG GACAA CTCTT AATCT G
ps4 AGGTG TTATC ATTCA TTTCA CTGAA *GGAGG CGGAG GTTGG TTCAG GTG*CT TTCAG GGAAA TTCCG CGGTG CTTA
ps5 GTGTC GAAGA TCGTG GGTCA TT*GTG GGTGG GTGTG GCTGG* TCCGA TCCGC GATCT GCTGA CGCTG GTTAG GT
ps6 ATCTG GCTAT GTTAG TCTTA TCACC ATGAC CGGAT GCCCC AAAA*G GTGGG TGGGT GGCGG* TAGAA TTTTG GTGTG T
ps7 GAGCC TCTGA TCAAT TAAAC ATTGT GTTAC T*GGTG GGTTT ATGCA GGTGG GTGGG* AACCA GGAAC ACTAT GTCCA
ps8 ATAGG TTTTG CTGGG GTAC*G GAGGT GGGCG GATGG TAGTG GTG*CC TGGCC CAGGA AAAAT TAGGG GCGAT GTCCA
ps9 ATCTA TGCTT ATTGG CCAAG AGTCG AATAA GGTGA TTC*GGG TAGGG CGGGC GG*TTC AATTA TTCGA CCTCG CTTTT
ps10 AATTG TGCAC AGCAG GACCG AATTT TTGAC TC*GGT GGGGC CATGG CGGGT GGGGC GGAG*A AATTT GGTCT AAGC
ps11 GATAA AGTTG TC*GGA TGGAT GCGGG TTGGG CTG*AT ATGAG AACTT TCAAG GGACA GACCT CAGGA TTCTA AATCG
ps12 CATCA TGAGT TT*GGG GAAGG GTCGG TGGGT G*CAAA AGTGG AATCC GCGAT TGATG GGGAC TCGTC ATCCC TAGGG A
ps13 CTTGG TCATT AGGCG AAGTA CCGGG GAGCG AACTA C*GGGC GGTGG GTACG GG*AAA GATTG TTCTG TAGTG ATGGT C
ps14 ATTTC GAGAG AGTAC *GGGTT GGGTT TGGGC AGG*AT AACAG TTTGG TGCTC TCTGG ATTAT GCCGA TGCCG GCC
ps16 TGATT GAACA CAATT CTGCA GACTC TGAGC AAGGG TATGG GGTTT TTGAC *GGGTG TGGTC GGCGG* TAACC TACAT C
ps17 TAGAT TTGTA CCC*GG GTTGG CGGGT GGTCT GTAAG GGG*TA CAAAA TCATG TGGGT AGTCT TTCTG CTTTG CCTGC AA
ps18 ATTTC *GAGGG AGTAC GGGTT GGGTT TGGGC AGG*AT AATAG TTTGG TGCTC TCTTG AAGTA TGCCG ATGCC GGCT
ps19 ATTAC AACAT AGTCA GGTTA TA*GGG CGGGA GGGTG G*TACA ACTGG CATTG TAAAT AGACG GATGC ATGTT GACTC
ps20 TAATC CTATG GTTTT TGCGA CTCGG CAATT CGTAA *GTGGG AGGGT GGTGG AG*ATA CGTAT GCTAG GTCAC GGGTA
ps21 ATTTC GAGAG AGTAC *GGGTA GGGTT TGGGC AGG*AT AATAG TTTGG GTCTC TCTGG AAGTA TGCCG ATGCC GCA
ps22 GATTA GCGGG TTAGT GGCAT TCGCT GCT*GA GGGGT GGGAG GTTGG* ATAAA TTGCG AATCC CATTA AAAGA TCC
ps24 AGGAT CGAGA ACAAT GACCA TGAAT GGAAA CATA*G AGGTG GGTGG TTTTT AGTGG G*TTGC ATTTA TGTTT ACATA C
ps25 GGTCC ATTCG GCTAT CCAGA C*GGGA GGGTG GGTGG ATTGG* ACACT TATGA ATGGA CCCTG CCCCC TTTCA TGTGC
ps26 ATCAT TAGGT AACTC GAC*GG GGTTG GGTCC GGGCG GTAGG* TTGAG TTTCC ATAAA ATCCG GTGAC GATTA TTATG A
ps30 ATAGG TTTTG CT*GGG GTACG GAGGT GGTCG GATGG* TAGAG GTGCC TGGCC CAGGA AAAAT TAGGG GCGAT GTCCA

FIGURE 2: Random regions of 24 short (**PS** family) aptamers that bound to NMM. Each aptamer appeared to have a single, very guanine-rich motif (the motifs containing between 55 and 78% guanine, with the balance being overwhelmingly thymine). No unambiguous consensus could be found between these sequences in terms of the positioning and number of contiguous guanines. The aptamers of the large (**P**) family also contained similar guanine-rich motifs, with at least one such motif per aptamer.

Table 1: Dissociation Constants[a]

NMM	MPIX	Fe(III)-MPIX	hemin	Ni(II)-MPIX	Zn(II)-MPIX
PS2					
0.5	1.5	2.8	1.4	1.7	1.8
0.5					
ST1					
0.8	3.6	2.6	1.7	3.6	4.9
0.7	3.0	2.1			
P7					
0.4	3.1	2.1			

[a] In micromolar.

Footprinting of Aptamer−Porphyrin Complexes

The precise binding sites of NMM and related porphyrins within the folded aptamers were investigated using footprinting experiments. Three approaches were attempted; one was methylation protection using dimethyl sulfate, which reveals the involvement of specific guanine N7 nitrogens in hydrogen bonding or in metal binding. The other two techniques were partial digestion by DNase I and DNA strand cleavage by bound hemin or mesohemin moieties in the presence of superoxide (KO_2). The data shown in Table 1 confirmed that MPIX, a number of its metalloderivatives, and hemin [iron(III) protoporphyrin] did bind to **PS2** and to the other aptamers tested, albeit with a lower affinity than did NMM. Iron(III) porphyrins, such as hemin or mesohemin, in the presence of strong oxidizing agents such as superoxide, are able to generate lesions in DNA, which lead to strand scission. We therefore reasoned that hemin (or mesohemin), bound to the aptamers, could be used to generate footprints *in situ* and help define "binding domains" on the basis of the proximity of specific DNA regions to the bound hemin.

Figure 3A shows the methylation protection patterns of **PS2** in different buffers, both in the presence and in the absence of NMM. When **PS2** was methylated in either TE or SB buffers (lanes 1 and 2), all of its guanines were reactive. However, methylation in the presence of 50 μM NMM in SB buffer gave a clear footprint (lane 3), with certain guanines (indicated by arrows) fully protected and others (indicated by arrowheads) enhanced. A very high concentration of NMM (1 mM, lane 5) appeared to protect all but the 3′-most and 5′-most guanines in the aptamer. Arguably, under these conditions, the DNA−porphyrin interaction was qualitatively different and, possibly, non-specific. Lanes 6−9 show footprints in the presence of 50 μM NMM but in buffers that lacked one or more components of SB [such as SB′: 50 mM potassium cacodylate (pH 7.0), 10 mM $MgCl_2$, and 5% DMSO; and SB′ + 100 mM NaCl]; in all of these cases, there was a partial footprint, with some of the guanines protected in lane 3 protected here and others not. The arrows next to lane 9 indicate the two most protected guanines in that lane, although the overall pattern is similar to that shown in lane 3. The pattern in lane 9 makes the interesting point that **PS2** is able to fold and form its NMM binding site in a magnesium-independent manner.

Lanes 0−3 of Figure 3B show **PS2** footprints generated by hemin and KO_2 (lane 0 contains no hemin; lanes 1−3 contain 30, 100, and 400 μM hemin respectively) and by mesohemin and KO_2 (lane 4 contains mesohemin at 400 μM). Whereas in the absence of bound hemin (lane 0) there is only a background DNA breakage pattern by KO_2, lanes 1−3 show the progressive appearance of a defined zone of cleavage, which superimposes well upon the methylation-protected zone (Figure 3A). Interestingly, the mesohemin

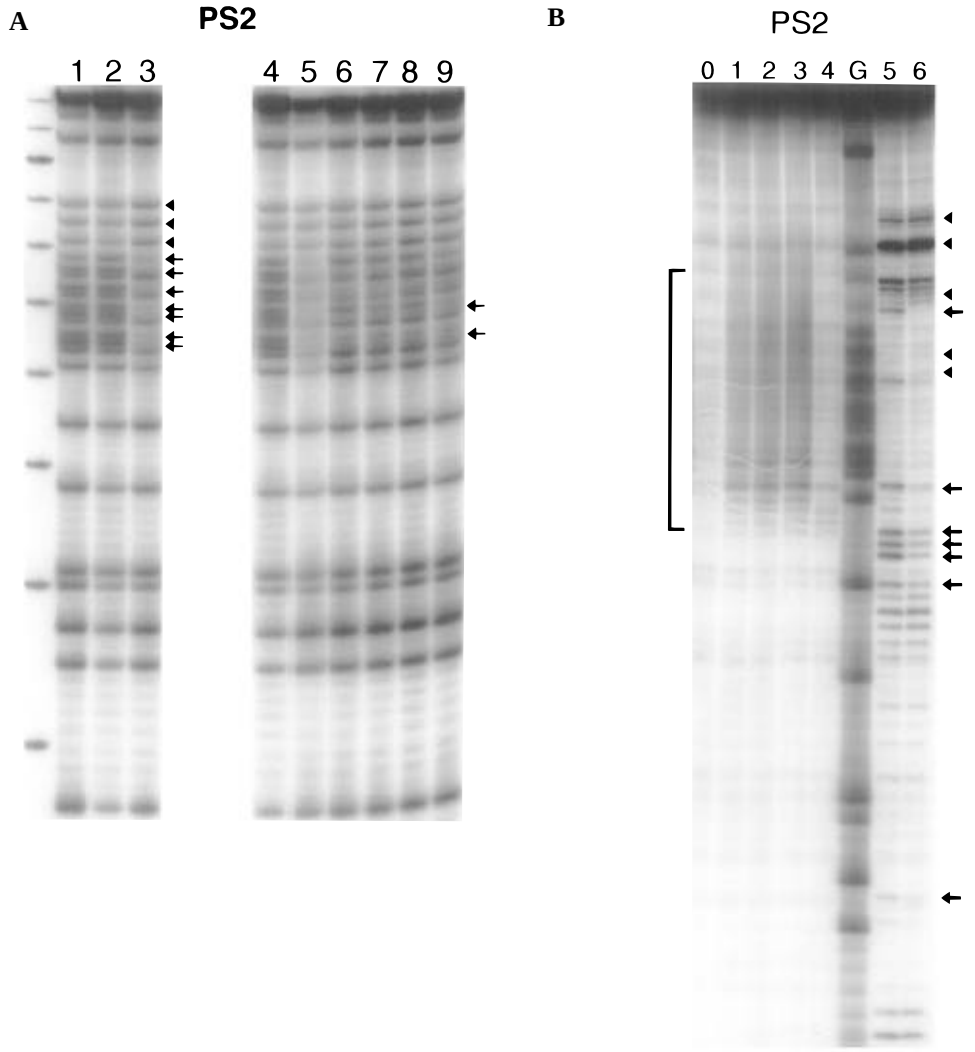

FIGURE 3: (A) Methylation protection of aptamer **PS2**, under different buffer conditions, and in the presence and absence of NMM: (lane 1) in TE buffer with no added NMM, (lane 2) in SB buffer with no added NMM, (lane 3) in SB with 50 μM NMM, (lane 4) as in lane 2, (lane 5) in SB with 1 mM NMM, (lane 6) in SB′ buffer [50 mM potassium cacodylate (pH 7.0), 10 mM $MgCl_2$, and 5% DMSO] with 100 μM NMM, (lane 7) in SB′ buffer with 1 mM NMM, (lane 8) in SB′ + 100 mM NaCl with 100 μM NMM, (lane 9) in SB′ + 100mM NaCl with 1 mM NMM. The extreme left-hand lane shows a 10 bp ladder (with the 100 b.p. band darker than the others). (B) DNase I, hemin/KO_2, and mesohemin/KO_2 footprinting of **PS2**: (lane G) Maxam−Gilbert guanine ladder of **PS2**, (lane 0) **PS2** without hemin treated with KO_2, (lanes 1−3) **PS2** in the presence of hemin (30, 100, and 400 μM, respectively) treated with KO_2, (lane 4) **PS2** in the presence of mesohemin (400 μM) treated with KO_2, (lane 5) **PS2** without NMM treated with DNase I, and (lane 6) **PS2** in the presence of NMM (100 μM) treated with DNase I.

cleavage zone (lane 4) is consistent with that of hemin (lane 3), but the cutting is of a much lower intensity.

Lanes 5 and 6 of Figure 3B show partial DNase I digests of **PS2**, in the absence (lane 5) and presence (lane 6) of bound NMM. Whereas there is broad agreement between the methylation protection and hemin/KO_2 cleavage zones, the DNase pattern differences between lanes 5 and 6 extend for tens of nucleotides *beyond* the borders of the putatively binding domain, indicating a significant tertiary structure change in the aptamer following the binding of NMM.

Figure 4 shows DMS as well as KO_2/hemin footprints for the aptamer **PS5**. **PS5** is unlike **PS2** (above) in that the aptamer itself, in SB buffer at room temperature, shows strong variation in the DMS reactivity of individual guanines in its G-rich motif (lane 1; G-rich motif indicated by a bracket). This suggests that these partially protected guanines are involved in hydrogen bonding with their N7 positions and that the G-rich motif of **PS5** (unlike **PS2**) is possibly folded into a modestly stable secondary/tertiary structure in SB buffer. The binding of NMM, in progressively higher added concentrations (lanes 2−4), however, does not simply enhance the pre-existing guanine protection pattern but alters this pattern in several ways, including enhancing the reactivity of certain guanines and further protecting others. Thus, in the *absence* of NMM, the motif shows the following reactivity pattern, gtgGGtgGGtgtGgctGgt, where guanines shown in uppercase are less reactive. The presence of NMM, however, gives rise to a more comprehensive protection pattern, with effectively all guanines in the motif underreacting; however, at a finer level, some guanine reactivities decrease, while others remain the same or are enhanced (one guanine *within* the motif, underlined above; another is located beyond the 3′-edge of the motif).

Figure 5A shows the methylation protection patterns of the larger aptamers **P3**, **P7**, and **P9**, in the absence and presence of 50 μM NMM. Single areas of protection (shown by brackets) are to be seen for each aptamer (Figure 5A).

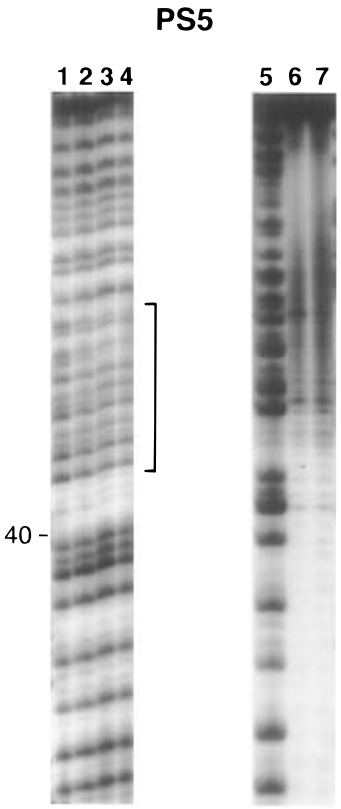

FIGURE 4: Methylation protection and hemin/KO_2 footprints of aptamer **PS5**: (lane 1) methylation pattern in SB buffer, in the absence porphyrin; (lanes 2−4) methylation pattern in SB buffer, in the presence of NMM (10, 100, and 300 μM, respectively); (lane 5) as lane 1; and (lanes 6and 7) in SB buffer with hemin and KO_2, treated with the DNA trapped within gel fragments, showing DNA recovered with no bound hemin (lane 6) and with bound hemin (lane 7) (see Materials and Methods).

The most notable feature of these footprints is that none of the these larger aptamers have *complete* protection of their binding site guanines, although partial protection is observed in all cases (lane 1). Addition of progressively higher concentrations of NMM, up to 800 μM, to **P3** still did not give a total protection of any guanine (data not shown). An interesting difference among these three aptamers was that, while **P7** appeared to require magnesium in the binding buffer in order to footprint with bound NMM (lane 2, showing incubation in SB buffer without magnesium), aptamers **P3** and **P9** gave footprints with NMM regardless of the presence (lane 1) or absence (lane 2) of magnesium in their binding buffers (*vide* **PS2** versus **PS5**, above). An additional feature of the pattern for **P3** is the following; the aptamer has at least two highly guanine-rich regions of comparable size and guanine content: from positions 35 to 55 (GcGGacGGGGcaGaGGGatG) and from 65 to 85 (GttGGGtGGtcatGtGGGtGG). However, the latter is the *only* motif that footprints (the 35−55 region, with no footprint, is not shown in Figure 5A, B), suggesting that it is not a sufficient condition simply to have a guanine-rich motif in order to generate an NMM-binding site. Similar conclusions can also be drawn about **P7** and **P9**.

Figure 5B shows the DNase I and hemin/KO_2 footprints for **P3**, **P7**, and **P9**. There were strong hemin/KO_2 footprints in all three cases (lane 2), essentially coinciding with the zones identified by methylation protection. Treatment of all three aptamers with KO_2 only, in the absence of bound hemin, gave low, background cleavages (lane 1). DNase footprinting of the aptamers in the presence and absence of NMM showed only modest differences, however, for all three aptamers; the few differences were located in the same general area as the other two classes of footprints. The modest DNase I cleavage differences for these large aptamers stand in marked contrast to those of **PS2** (Figure 3B).

*Interactions of **PS2** with Porphyrins, Metalloporphyrins, and ATP*

We investigated whether porphyrins such as MPIX, as well as a host of metalloporphyrins derived from MPIX, gave footprinting patterns comparable to or different from that of NMM. Figure 6A shows the DMS footprinting patterns of aptamer **PS2** in the presence of a variety of porphyrins and metalloporphyrins, as well as ATP (which has been proposed recently to have a guanine quartet-containing binding motif formed by DNA; Huizenga & Szostak, 1995). Footprints in the presence of three different concentrations of NMM (50, 5, and 0.5 μM NMM, respectively, in lanes 2−4) indicate that the lower concentrations gave partial footprints, whereas their final form was reached only in the 50 μM incubation (the protected area is indicated with a bracket). Hemin, MPIX, and the Fe(III), Zn(II), Ni(II), and Cu(II) derivatives of MPIX did not footprint at all in 50 μM incubations of the various porphyrins. Only Co(III)-MPIX showed a general and comprehensive protection of guanines in the binding motif (including those guanines that were not protected by 50 μM NMM, although resembling the pattern found with 1 mM NMM; Figure 3A). It is conceivable that Co(III)-MPIX, like NMM at high concentrations, shows a nonspecific mode of binding, one which protects all of the guanines in the binding motif from methylation. As in Figure 3A, NMM in SB′ buffer gave a significant protection, and this was found even in the magnesium-free TE buffer. This is an interesting point of difference between **PS2** and **PS5**, in that the former seems to fold to produce the NMM-binding site even in the absence of magnesium, whereas **PS5** requires magnesium.

ATP, even at high concentrations (0.5 mM), did not give a footprint.

A Small DNA Aptamer

Both the methylation protection and hemin/KO_2 footprinting data on the five clones examined indicate that short, well-defined G-rich domains (a single, contiguous sequence of nucleotides in each aptamer) are responsible for binding porphyrins. The DNase I digestion data, however, at least in the case of **PS2**, indicate that changes in conformation and accessibility to the enzyme can extend well beyond the domains defined by the other two footprinting techniques. It was therefore interesting to test whether an isolated G-rich domain (as defined by the 5′- and 3′-limits established by the hemin/KO_2 and methylation protection cleavages on **PS2**), shorn of its neighboring sequences, could still bind NMM.

A short, 25-nucleotide oligomer, **ST1**, encompassing the G-rich domain of **PS2**, with the sequence 5′-AACGT GGGAG GGCGG TGGTG TTGAA, was synthesized. Dissociation constants of different porphyrins with **ST1** were measured and methylation protection and KO_2 cleavages carried out in the presence and absence of porphyrins. The

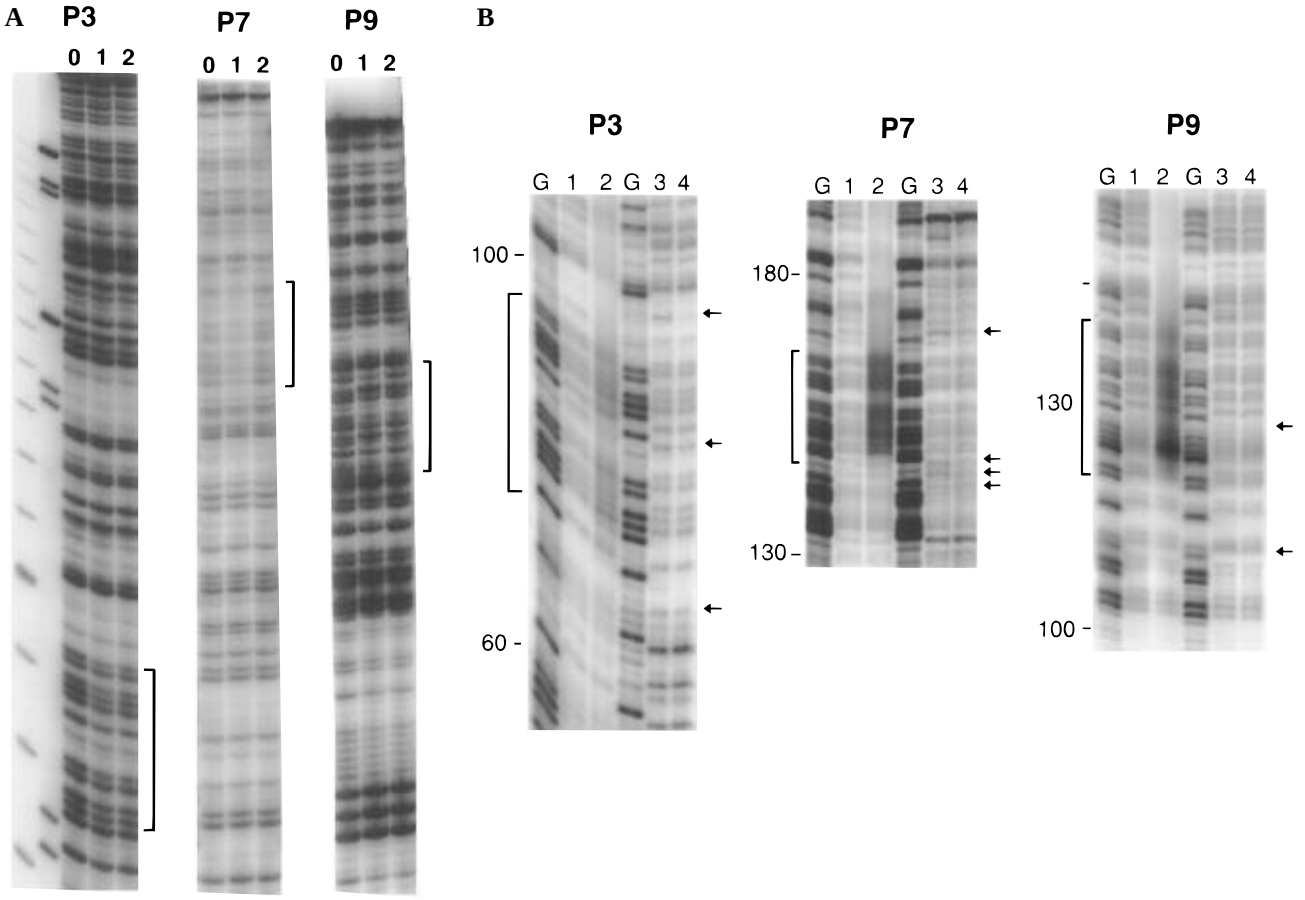

FIGURE 5: (A) Methylation protection patterns of aptamers **P3**, **P7**, and **P9**: (lane 0) in SB buffer, in the absence of NMM; (lane 1): in SB buffer, in the presence of NMM; and (lane 2) in SB buffer lacking magnesium chloride, in the presence of NMM. The protected regions in lanes 1 and 2 are indicated with brackets. (B) Hemin/KO_2 and DNase I footprints of aptamers **P3**, **P7**, and **P9**: (lane G) Maxam−Gilbert guanine ladders, (lane 1) aptamers without hemin treated with KO_2, (lane 2) aptamers in the presence of hemin (400 μM) treated with KO_2, (lane 3) aptamers without NMM treated with DNase I, and (lane 4) aptamers in the presence of NMM (100 μM) treated with DNase I.

results indicated that **ST1** was competent to bind porphyrins almost as strongly as the parent aptamer **PS2** (Table 1), but not in an identical manner. Figure 6B (left) shows the methylation protection patterns of **ST1** with different porphyrins; the arrows on the left indicate those guanines that are protected in the presence of 50 μM NMM (whereas arrowheads indicate guanines that are enhanced). Comparison of Figure 6B with Figure 3A indicates that the **ST1** pattern has fewer protected guanines (and each guanine protected to a lesser extent) than the **PS2** pattern. However, like **PS2**, **ST1** is not footprinted by incubations with 50 μM MPIX, mesohemin [Fe(III)-MPIX], or hemin. In addition, Co(III)-MPIX induces a wholesale protection of all but the outermost guanines of **ST1**, as it does in **PS2**.

Treatment of **ST1** with hemin/KO_2 showed cleavage of the entire oligomer (data not shown), as expected.

Like **PS2** (but unlike **PS5**), **ST1**, in the absence of porphyrin, did not show much variation in the DMS reactivity of its individual guanines (lane SB, Figure 6B) in SB buffer at room temperature. However, guanine-rich telomeric oligomers similar in sequence to **ST1** have been shown to form intramolecularly folded G·G base pair- and guanine quartet-containing structures under conditions of high salt and/or low temperature [Henderson et al., 1987; reviewed recently by Williamson (1993, 1994) and Sundquist (1993)]. We therefore tested whether **ST1** at 0 °C (comparable to **PS5** at room temperature) gave a modulated G-reactivity pattern with dimethyl sulfate and whether the binding of NMM simply intensified this pattern or gave rise to a different methylation protection pattern (as in the case of **PS5**). Comparison of the SB 20 °C and SB 0 °C lanes in Figure 6B shows that at 0 °C some guanines were indeed under-reactive compared to the situation at 20°; however, methylation in the presence of NMM at 0 °C gave a pattern different from both of the others (arrows indicate protections induced by NMM and arrowheads enhancements).

These mutually consistent data from **PS5** and **ST1** indicate, therefore, that it is probably not the case that NMM binds to a pre-existing higher-order structure formed by the different G-rich motifs; rather, the presence of NMM appears to induce distinctive folding patterns for the binding motifs.

Gel Mobilities of Aptamer−NMM Complexes

The footprinting/protection experiments above indicate that NMM binding influences the overall folded structure of a number of aptamers. This is indicated not only by changes in the methylation patterns of guanines within the binding motifs but also by changes in the DNase I cutting patterns, which often (as in the case of **PS2**) extend significantly beyond the binding motif in both the 5′- and 3′-directions. We ran the aptamers **PS2** and **PS5**, with added and no added NMM, in a nondenaturing, magnesium-containing gel, to see if there were any gross differences in gel mobility of the aptamers in the presence versus the absence of NMM. Figure 7 shows that both aptamers showed a discernably slower mobility in the presence of added NMM (NMM added

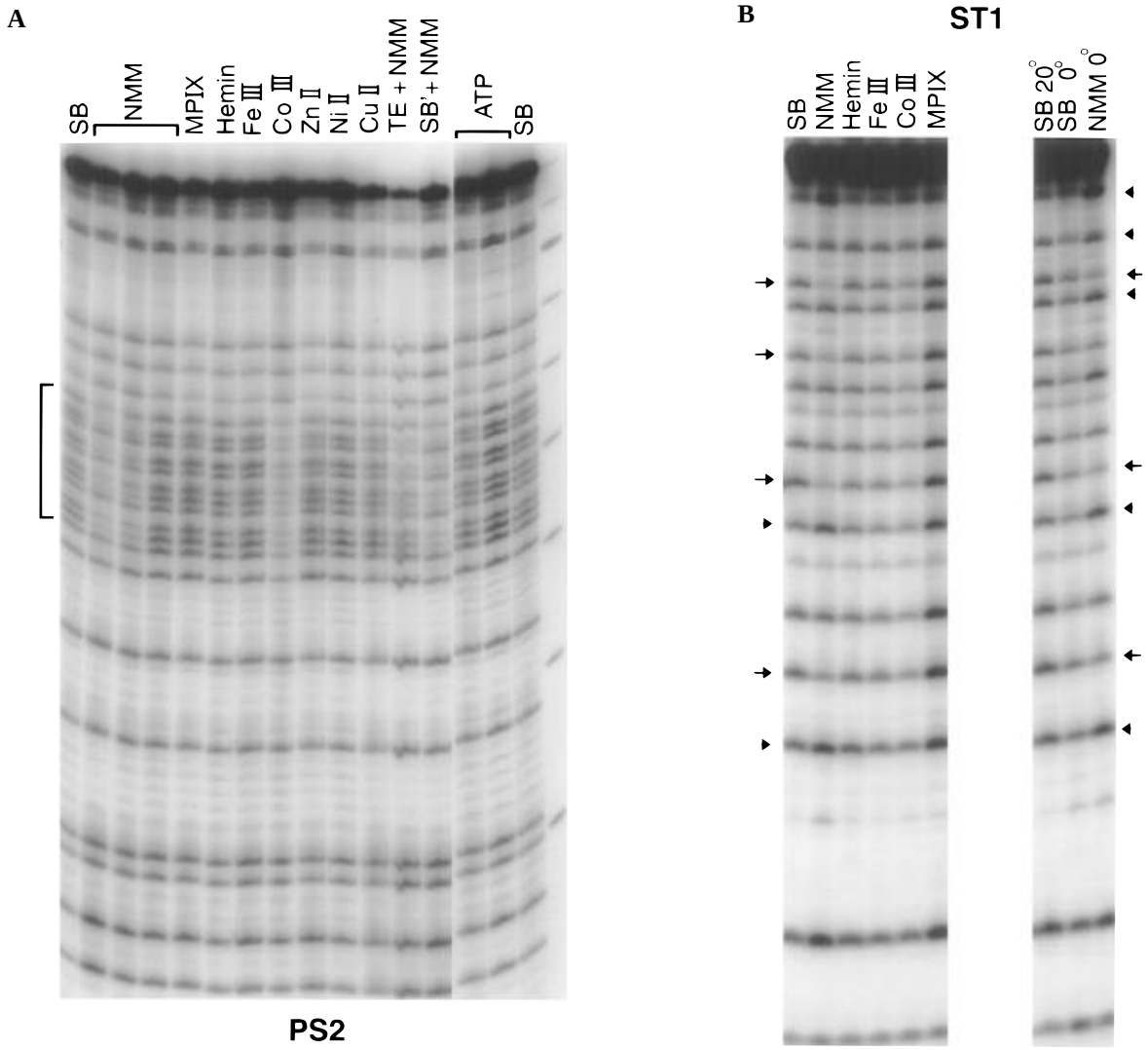

FIGURE 6: (A) Methylation protection patterns induced in **PS2** by porphyrins and metalloporphyrins. **PS2** (from left) in SB buffer in the absence of porphyrins; in SB buffer in the presence of 50, 5, and 0.5 μM NMM, respectively; in SB with 50 μM each of MPIX, hemin, Fe(III)-MPIX, Co(III)-MPIX, Zn(II)-MPIX, Ni(II)-MPIX, and Cu(II)-MPIX; in TE buffer with 50 μM NMM; in SB′ buffer with 50 μM NMM; in SB with 50 and 500 μM ATP, respectively; and in SB without porphyrins. The extreme right-hand lane shows a 10 bp ladder. (B) Methylation protection pattern of the short aptamer **ST1** with different porphyrins (left) and (Right) comparison of guanine reactivity in the absence of NMM at 0 °C, relative to its presence, also at 0 °C (rght): (left panel) **ST1** (1) in SB in the absence of porphyrins; with added (2) NMM, (3) hemin, (4) mesohemin [Fe(III)-MPIX], (5) Co(III)-MPIX, and (6) MPIX itself. The complete arrows indicate protection of guanines in lane 2 as compared to lane 1; arrowheads indicate enhancements of guanines: (right panel) (7) as in lane 1; (8) as in lane 1, but probed at 0 °C; and (9) as in lane 2, but probed at 0 °C.

to the relevant samples before loading but not present in the gel buffer). The larger aptamers also showed this shift, although to a lesser extent. NMM itself would be expected to contribute one to two negative charges from its carboxylic acid side chains to the aptamer−NMM complexes; however, the mobility differences observed are conceivably too large to be explained simply in terms of an increase in the overall negative charge of the complexes, from 120 to 121 or 122. It therefore appears that NMM binding gives rise to a moderate change in the overall tertiary structure of the binding aptamers, which is reflected in altered gel mobilities.

Interestingly, **ST1** showed a relative gel shift in the presence of NMM that was not much larger than that of the parent aptamer **PS2** (data not shown). **ST1** is unusual in that it has no extraneous nucleotides other than the porphyrin binding site, so any structural changes induced by porphyrin binding are inherently "local" rather than potentially "global", as in the case of **PS2**.

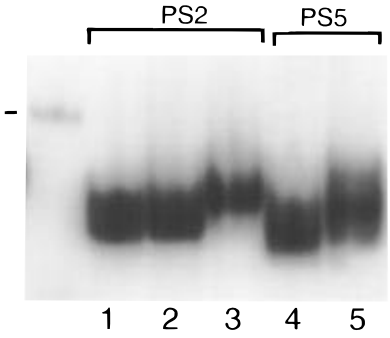

FIGURE 7: Mobilities of **PS2** and **PS5**, in the absence and presence of NMM, in a nondenaturing gel run at 4 °C in TB buffer + 10 mM KCl + 5 mM $MgCl_2$: (lane 1) **PS2** in TE buffer, (lane 2) **PS2** folded in SB buffer, (lane 3) **PS2** folded in SB and treated with 100 μM NMM, (lane 4) **PS5** folded in SB, and (lane 5) **PS5** folded in SB and treated with 100μM NMM. The extreme left lane shows a double-stranded DNA marker (48 bp).

```
...cgtg GGa-- gGG cg- GtgG t-- Gtt gactg...
  ...tGt GGg-t GGg t-- GtGG ct- GGt ccgat...
...gttg GGt-- gGt cat GtGG Gt- GGt tattc...
...gGcg GGc-- gGt tgG GtgG tta tGt aacGg...
...Gatc GG cag gGG at- GtGg t-g GGt atGGgccGa...
```

FIGURE 8: Comparison of methylation protection patterns for the NMM-binding sequences within aptamers (from above): **PS2**, **PS5**, **P3**, **P7**, and **P9**. The guanines that show a greater level of protection in the presence of NMM are shown in uppercase, whereas those that are not are shown in lowercase. The underlined regions indicate zones defined by footprinting with hemin and KO_2.

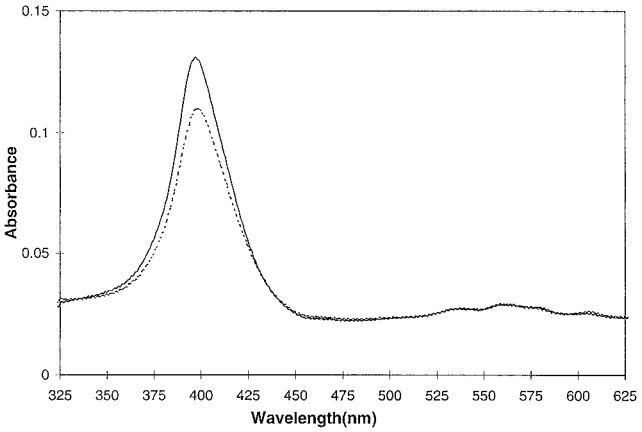

FIGURE 9: Ultraviolet−visible absorption spectra of 1 μM NMM, in the presence (dotted line) and in the absence (continuous line) of **PS2** (5 μM).

A Sequence Consensus for the Structure of the Binding Site

Figure 8 summarizes the methylation and DNase I-footprinting data for the five aptamers we have examined in detail. Guanines shown in uppercase are those that are found to be less reactive to dimethyl sulfate in the presence of NMM than in its absence (although, as stated earlier, in the case of **PS5**, some guanines shown to be "unaffected" by the presence of NMM in Figure 8 were already underreactive in the absence of NMM; Figure 4). Figure 8 shows that a reasonable alignment of four separate stretches of one to three guanines each can be made. However, whether this represents a structurally meaningful "consensus" cannot be confirmed at this point. It is conceivable that there are a number of closely related tertiary structures formed by the guanine-rich sequences, any of which can constitute a reasonable binding site for NMM. More detailed structural work will be required before the precise requirements for a binding site can be elucidated. We are currently carrying out several such experiments.

Spectroscopic Studies of Aptamer−NMM Complexes

We investigated the mode of binding of NMM to the folded aptamers using ultraviolet−visible absorption and circular dichroism spectroscopy.

UV Absorption Spectroscopy. Figure 9 shows the ultraviolet−visible absorption spectra (from 325 to 625 nm and showing the Soret and visible absorption regions of NMM) of 1 μM NMM in the presence (dotted line) and absence (continuous line) of 5 μM **PS2**. The presence of the excess aptamer induces an ~10% hypochromicity in the Soret absorption but an almost negligible shift (~1 nm toward the red) of the absorption maximum. The visible bands appear not to be significantly affected, in terms of both hypochromicity and the position(s) of the absorption maxima. This overall pattern is significantly different from those seen in any of the proposed three modes of binding of cationic porphyrins to double-stranded DNA (Carvlin et al., 1982).

Circular Dichroism Spectroscopy. The CD spectra in the presence and absence of NMM were examined for the small aptamer **ST1** and for **PS2**. In the DNA absorption region, **ST1** did not give a significant CD signal, even at 0 °C, suggesting that it is essentially nonhelical in terms of its secondary and tertiary folding. The presence of added NMM, however, did not induce a spectrum in the DNA absorption region. Undoubtedly, **ST1** bound to NMM is more structured than it is in the absence of NMM; however, the overall helical content for this small DNA molecule may not be very great, even in the presence of NMM. **PS2** gave a standard B-DNA CD spectrum on its own, and this did not substantially change in the presence of NMM. Undoubtedly, folded **PS2** has elements of double helix within it, although these regions may not be relevant to NMM binding. In both the Soret and visible absorption regions for the porphyrin, neither **PS2** nor **ST1** gave rise to induced CD spectra.

DISCUSSION

DNA Sequences That Bind NMM. It is not yet clear whether the sequence consensus derived from the sequence comparisons and from methylation protection studies, shown in Figure 8, has more than a very general relevance to the folded structure actually responsible for binding NMM. This possibility is raised by inspection of the methylation-protected guanines of individual aptamers. While the derived consensus sequence does incorporate a high proportion of these protected guanines, in each case there exist a number of others that sit outside of the consensus region. It is therefore conceivable that the postulated G quartet-mediated binding site formed by *each* aptamer is distinctive, giving rise to the extreme possibility that *any* guanine quartet-containing complex would bind NMM and the other porphyrins. Whether this is true is currently under active investigation; however, preliminary data indicate an extremely marginal hemin/KO_2 footprinting of a G quartet-contaning "synapsable DNA" complex (Venczel & Sen, 1995).

Possible Role for Guanine Quartets. Guanine quartet-containing DNA and RNA structural motifs ("G-DNA" and "G-RNA") have recently emerged as relatively common motifs for the binding of different classes of small molecules (ATP/adenosine; riboflavin) as well as proteins (thrombin). DNA aptamers specific for thrombin have been shown by X-ray diffraction and by NMR to contain G quartets (Macaya et al., 1993; Wang et al., 1993a,b; Padmanabhan et al., 1993; Schultze et al., 1994); G quartet-containing models have also been proposed for adenosine/ATP binders (DNA aptamers; Huizenga & Szostak, 1995) and riboflavin binders (RNA aptamers; Lauhon & Szostak, 1995). These aptamers are among the most strongly bound to their respective target molecules, with measured dissociation constants as low as 25 nM (in the case of thrombin; Bock et al., 1992). The RNAs that bind flavin have a sequence consensus of $N_{0-2}GGN_{1-2}GGN_{1-2}GGN_{1-2}GGN_{1-3}$, which has been modeled as a folded structure containing two consecutive guanine quartets; a similar structure has been shown with the high-

resolution structural studies for the thrombin-binding DNA aptamer (Bock et al., 1992), whose consensus sequence is d(GGtTGGN_{2-5}GGtTGG) (in which G and T are constant, N is any nucleotide, and t represents a bias toward thymine). The adenosine/ATP-binding sequence DNA aptamers have been proposed to fold to give two adjacent G quartets, as well as two consecutive Watson−Crick duplexes.

Some of the porphyrin-binding aptamers described in this study, including **PS5** (and **ST1** at 0 °C), show degrees of methylation protection of some of their binding site guanines in the absence of NMM; with bound NMM, a significantly *different* protection pattern is produced, which appears, in a number of cases, to be potassium-dependent (data not shown). These data are consistent with the involvement of the protected guanines in forming guanine−guanine Hoogsteen hydrogen bonds, likely within the context of guanine quartets (Sen & Gilbert, 1988, 1990; Williamson et al., 1989; Sundquist & Klug, 1989). NMM appears to induce the *complete* protection of certain guanines in **PS2**, **PS5**, and **ST1**, whereas in the absence of NMM, these aptamers show only very limited intrinsic protection of any guanines, suggesting that, whatever guanine-mediated folded structures might exist, they are probably labile. It is conceivable that the presence of NMM provides a template for the formation of further G−G interactions, with the NMM molecule effectively playing a role in creating its own binding site.

Mode of NMM Binding. How might NMM bind to folded DNA structures that possibly contain one or more guanine quartets? Both porphyrins and guanine quartets are large and substantially planar aromatic systems; it might be expected that the two might interact via the intercalation of porphyrins between successive guanine quartets. However, our ultraviolet−visible absorption and circular dichroism spectra suggest that classic intercalation is probably not the mode of interaction between NMM and the aptamers.

A number of changes in physical and spectroscopic properties associated with the binding of ligands by double-stranded DNA have been recognized as defining for an intercalative mode of binding [reviewed in Pasternack et al. (1983) and Chaires (1990)]. These include: DNA helix stabilization against thermal denaturation, helix unwinding, and an increase in solution viscosity as a consequence of the DNA lengthening. These, unfortunately, are not properties that can be tested with single-stranded aptamers. Other expected features of porphyrin intercalation are as follows: substantial hypochromicity and red shifts of DNA ultraviolet absorption bands as well as that of the Soret absorption of the porphyrin and induced optical activity in the visible region for the porphyrin, as well as changes in the ellipticity of DNA in the near-ultraviolet. Thus, Carvlin and Fiel (1983) reported for the intercalation of mesotetra(3-*N*-methylpyridyl)porphine (T3MPyP) into calf thymus DNA a substantial red shift of the porphyrin visible band, from ∼416 to ∼433 nm, and a large hypochromicity of ∼47%.

We measured ultraviolet−visible absorbance and circular dichroism spectra for NMM in the absence and presence of excess aptamer **PS2** and found an ∼10% hypochromicity in the porphyrin Soret absorption and a very small red shift (<1 nm). The visible absorption of the porphyrin appeared largely unchanged. In addition, no significant change in the circular dichroism spectrum of the DNA and no induced CD spectrum around the Soret and visible absorption regions of the porphyrin were found.

These observations suggest that the interaction of NMM with the aptamer **PS2** is not by a classic intercalation mechanism. As discussed earlier, it is likely that the porphyrin binding site (at least when NMM is bound) contains one or more guanine quartets. The interaction of DNA-binding drugs with guanine quartets has been studied in one single instance, the binding of ethidium bromide to the parallel tetraplex formed by the self-association of dT_4G_4 (Guo et al., 1992). In that study, ethidium was found to intercalate in a classical manner between G quartets (giving rise to a red shift of ∼35 nm and hypochromicity of ∼20% for the ethidium visible absorption band). An intercalative mode of binding between adjacent G quartets is therefore theoretically possible for porphyrins; however, NMM appears not to bind in this way to the aptamers we have examined. The lack of an induced CD spectrum for the porphyrin visible absorption when bound to **PS2** is also significant in that it suggests that possibly only one (or a very few) molecule of porphyrin binds to each molecule of **PS2**.

Relevance to the RNA World. The definition of a binding site within folded single-stranded DNA for a naturally occurring anionic porphyrin has important theoretical connotations. Ribozymes that have been found to date in nature are relatively narrow in the range of their catalytic activities, and extant ribozymes probably represent a vestige of a previously much larger group of enzymes, which catalyzed a broad range of chemical reactions connected with metabolism. The lack of a diversity of functional groups within RNA (and DNA) as compared to proteins has been noted (White, 1976; Gilbert, 1986; Benner et al., 1989). It is therefore of interest that DNA is able to form high-affinity and specific binding sites for naturally occurring anionic porphyrins and their metalloderivatives, for the latter currently constitute a large and verstatile class of cofactors and prosthetic groups and could have been recruited by early RNA catalysts to carry out specialized metabolic functions.

Future Experiments. The isolation of DNA aptamers that bind to the porphyrin NMM with a high affinity and to other, related porphyrins with lesser affinity will permit us to examine whether such aptamers can carry out a catalytic function similar to that of the antibodies described by Cochran and Schultz (1990a), that of inserting metal ions into the porphyrin MPIX. Preliminary studies indicate chelatase activity for some of our clones.

The relatively loose sequence consensus required for the binding of the various porphyrins and metalloporphyrins (including hemin and mesohemin) examined by us suggests that different aptamers interact with porphyrins with similar but nonidentical geometries. It is therefore conceivable that some of the aptamer−hemin or aptamer−mesohemin complexes, as well as other metalloporphyrin−aptamer complexes, might be able to catalyze, in the presence of an appropriate oxidizing agent, the chemistries associated with peroxidase or monooxygenase enzymes. One of the catalytic antibodies for chelatase activity isolated by Cochran and Schultz (1990a) also showed peroxidase activity when bound to mesohemin (Cochran & Schultz, 1990b). We are actively investigating all of these possibilities.

ACKNOWLEDGMENT

We thank colleagues at Simon Fraser University for their help, in particular Drs. Andrew Bennet and Charles Boone.

REFERENCES

Bartel, D. P., & Szostak, J. W. (1993) *Science 261*, 1411−1418.
Benner, S. A., Ellington, A. D., & Traver, A. (1989) *Proc. Natl. Acad. Sci. U.S.A. 86*, 7054−7058.
Bock, L. C., Griffin, L. C., Latham, J. A., Vermass, E. H., & Toole, J. J. (1992) *Nature 355*, 564−566.
Bromley, S. D., Ward, B., & Dobrowiak, J. C. (1986) *Nucleic Acids Res. 14*, 6875.
Carvlin, F. J., & Fiel, R. J. (1983) *Nucleic Acids Res. 11*, 6121.
Carvlin, F. J., Mark, R. J., Fiel, R. J., & Howard, J. C. (1983) *Nucleic Acids Res. 11*, 6141.
Chaires, J. B. (1990) *Biophys. Chem. 35*, 191−202.
Cochran, A. G., & Schultz, P. G. (1990a) *Science 249*, 781−783.
Cochran, A. G., & Schultz, P. G. (1990b) *J. Am. Chem. Soc. 112*, 9414−9415.
Connell, G. J., Illangsekare, M., & Yarus, M. (1993) Biochemistry 32, 5497−5502.
Dailey, H. A., & Fleming, J. E. (1983) *J. Biol. Chem. 11*, 453.
Ellington, A. D., & Szostak, J. W. (1990) *Nature 346*, 818−822.
Ellington, A. D., & Szostak, J. W. (1992) *Nature 355*, 850−852.
Famulok, M., & Szostak, J. W. (1992) *J. Am. Chem. Soc. 114*, 3990−3991.
Fiel, R. J. (1989) *J. Biomol. Struct. Dyn. 6*, 1259−1283.
Gibbs, E. J., Maurer, M. C., Zhang, J. H., Reiff, W. M., Hill, D. T., Maliska-Blaskiewicz, M., McKinnie, R. E., Liu, H. Q., & Pasternack, R. F. (1988) *J. Inorg. Biochem. 32*, 39−65.
Gilbert, W. (1986) *Nature 319*, 618.
Guo, Q., Lu, M., Marky, L. A., & Kallenbach, N. R. (1992) *Biochemistry 31*, 2451−2455.
Henderson, E. R., Hardin, C. C., Wolk, S. K., Tinoco, I., Jr., & Blackburn, E. H. (1987) *Cell 51*, 899−908 .
Hirao, I., & Ellington, A. D. (1995) *Curr. Biol. 5*, 1017−1022.
Huizenga, D. E., & Szostak, J. W. (1995) *Biochemistry 34*, 656−665.
Jelinek, D., Lynnot, C. K., Rifkin, D. B., & Janjic, C. (1993) *Proc. Natl. Acad. Sci. U.S.A. 90*, 11227−11231.
Jelinek, D., Green, L. S., Bell, C., & Janjic, C. (1994) *Biochemistry 33*, 10450−10456.
Jenison, R. D., Gill, S. C., Pardi, A., & Polisky, B. (1994) *Science 263*, 1425−1429.
Joyce, G. F. (1994) *Curr. Opin. Struct. Biol. 4*, 331−336.
Lauhon, C. T., & Szostak, J. W. (1995) *J. Am. Chem. Soc. 117*, 1246−1257.
Lavallee, D. K. (1988) *Mol. Struct. Energ. 9*, 279.
Lorsch, J. R., & Szostak, J. W. (1994) *Biochemistry 33*, 973−982.
Lu, M., Guo, Q., Pasternack, R. F., Wink, D. J., Seeman, N. C., & Kallenbach, N. R. (1990) *Biochemistry 29*, 570−578.
Macaya, R. F., Schultze, P., Smith, F. W., Roe, J. A., & Feigon, J. (1993) *Proc. Natl. Acad. Sci. U.S.A. 90*, 3745−3749.
Marzilli, L. G. (1990) *New J. Chem. 14*, 409−420.
Nussbaum, J. M., Newport, M. E., Mackie, M., & Leontis, N. B. (1994) *Photochem. Photobiol. 59*, 515−528.
Padmannabhan, K., Padmanabhan, K. P., Ferrara, J. D., Sadler, J. E., & Tulinsky, A. (1993) *J. Biol. Chem. 268*, 17651−17654.
Pasternack, R. F., Gibbs, E. J., & Villafranca, J. J. (1983) *Biochemistry 22*, 2406.
Sassanfar, M., & Szostak, J. W. (1993) *Nature 364*, 550−552.
Schultz, P. G., & Lerner, R. A. (1995) *Science 269*, 1835−1842.
Schultze, P., Macaya, R., & Feigon, J. (1994) *J. Mol. Biol. 235*, 1532−1547.
Sen, D., & Gilbert, W. (1988) *Nature 334*, 364−366.
Sen, D., & Gilbert, W. (1990) *Nature 344*, 410−414.
Sundquist, W. I. (1993) *Curr. Biol. 3*, 893−895.
Sundquist,W. I., & Klug, A. (1989) *Nature 342*, 825−829.
Szostak, J. W. (1993) *Trends Biochem. Sci. 17*, 89−93.
Tuerk, C., & Gold, L. (1990) *Science 249*, 505−510.
Tuerk, C., MacDougal, S., & Gold, L. (1992) *Proc. Natl. Acad. Sci. U.S.A. 89*, 6988−6992.
Venczel, E. A., & Sen, D. (1995) *J. Mol. Biol.* (in press).
Wang, K. Y., Krawczyk, S. H., Bischofberger, N., Swaminathan, S., & Bolton, P. H. (1993a) *Biochemistry 32*, 11285−11292.
Wang, K. Y., McCurdy, S., Shea, R. G., Swaminathan, S., & Bolton, P. H. (1993b) *Biochemistry 32*, 1899−1904.
Ward, B., Skorobogaty, A., & Dobrowiak, J. C. (1986) *Biochemistry 25*, 6875.
White, H. B., III (1976) *J. Mol. Evol. 7*, 101−104.
Williamson, J. R. (1993) *Curr. Opin. Struct. Biol. 3*, 357−362.
Williamson, J. R. (1994) *Annu. Rev. Biophys. Biomol. Struct. 23*, 703−730.
Williamson, J. R., Raghuraman, M. K., and Cech, T. R. (1989) *Cell 59*, 871−880.

BI960038H